Polymer Chemistry

Accepted Manuscript

ROYAL SOCIETY OF CHEMISTRY

www.rsc.org/polymers

Journal Name

RSCPublishing

ARTICLE

Effect of different chalcogenophenes in isoindigo-based conjugated copolymer on photovoltaic properties

Eui Hyuk Jung, Seunghwan Bae, Tae Woong Yoo and Won Ho Jo*

Cite this: DOI: 10.1039/x0xx00000x

Received 00th January 2012,
Accepted 00th January 2012

DOI: 10.1039/x0xx00000x

www.rsc.org/

New low bandgap conjugated copolymers based on isoindigo and three different chalcogenophenes (thiophene, selenophene and tellurophene) were synthesized (denoted as PIT, PISe and PITe, respectively) to investigate the effect of different chalcogenophene on their photovoltaic properties. PISe and PITe show lower bandgap and deeper HOMO energy levels as compared to PIT. The solar cell device based on PISe blended with $PC_{61}BM$ exhibits a promising PCE of 5.72% with a J_{SC} of 10.21 mA cm^{-2}, while PITe shows the lowest PCE of 1.16% with the lowest J_{SC} of 2.51 mA cm^{-2} because of its coarse morphology although the field-effect hole mobility of PITe is highest due to higher crystallinity than others.

Introduction

Solution-processed polymer solar cells (PSCs) have attracted much attention as a renewable energy source due to promising advantages such as low cost, light weight and flexibility.[1–6] In the past decade, the power conversion efficiency (PCE) of PSCs was largely improved by development of novel conjugated polymers with high carrier mobility and broad absorption of the solar spectrum especially at long wavelengths region.[7–9] One of the most effective method to synthesize such novel conjugated polymers is to copolymerize an electron-donating monomer (D) with an electron-accepting monomer (A). Many electron-accepting monomers have been developed for D–A type low bandgap copolymers over the past decade.[9–12]

Isoindigo has recently been used as an A unit for D–A type copolymers, because isoindigo contains two strong electron-withdrawing lactam rings with planar conjugated structure.[13–26] It has been reported that isoindigo-based polymers exhibit high absorption coefficient, broad absorption and deep highest occupied molecular orbital (HOMO) energy level.[14–26] Since Reynold *et al*.[13] first reported an isoindigo-based small molecule for photovoltaic application, isoindigo-based polymers have also been synthesized and used for photovoltaics.[14–26] Recently, the devices fabricated from isoindigo-based polymers have achieved high PCEs up to 8.2%.[15,17]

It has been known that heterocyclic aromatic rings with different chalcogens (the chemical elements in group 16) show different electrical, photophysical and electrochemical properties.[27] Thiophene-based conjugated polymers have been mostly used for photovoltaic applications,[9-12] although other chalogenophene-based polymers also have strong potential for optoelectronic applications. Selenophene-based semiconducting organic compounds have several advantages over thiophene-based ones: (1) selenophene-based conjugated polymers have narrower optical bandgap than thiophene-based ones,[28–33] because selenophene-based polymer backbone is better planar than thiophene-based one due to shorter inter-ring C–C bond between selenophene and the adjoining molecule,[27,34] and (2) selenophene-containing molecule has stronger intermolecular interaction than the thiophene-containing counterpart because selenium atom in selenophene is more easily polarized than sulfur atom in thiophene.[27,34] Hence, it is expected from above properties that selenophene-based conjugated polymers exhibit broader photon absorption and higher crystallinity. Likewise, since tellurium has stronger polarizability than sulfur and selenium, tellurophene-based polymers show bathochromic shift and higher crystallinity compared to that of thiophene- or selenophene-based polymer.[35–43] These advantageous properties of selenophene and tellurophene provide a strong potential for promising building block for high-performance conjugated polymers.

In this study, we synthesized three isoindigo-based D–A type conjugated copolymers (PIT, PISe, PITe) with three different chalcogenophenes (thiophene, selenophene and tellurophene) and compared their photovoltaic properties. The two copolymers (PISe and PITe) containing selenophene and tellurophene show bathochromic shift and lower band-gap as compared to its thiophene analogue (PIT). The solar cell

fabricated from PISe:[6,6]-phenyl-C_{61}-butyric acid methyl ester ($PC_{61}BM$) blend exhibits a promising PCE of 5.72% with a J_{SC} of 10.21 mA cm^{-2}, a high V_{OC} of 0.95 V and a fill factor of 59%. Consequently, it is concluded that selenophene is the most promising building block among the three chalcogenophens for high performance semiconducting conjugated polymers.

Experimental

Materials

All chemicals were purchased from Sigma-Aldrich, Alfa-Aesar and TCI chemicals, and used without further purification. The following compounds were synthesized according to the procedures reported previously: 6,6'-dibromo-*N*,*N*'-(2-hexyldecyl)isoindigo,[21,44] tellurophene,[45–47] and 2,5-bis(trimethyl-stannyl)chalcogenophene.[48,49]

Synthesis of copolymers

For synthesis of PIT, a mixture of (*E*)-6,6'-dibromo-1,1'-bis(2-hexyldecyl)-[3,3'-biindolinylidene]-2,2'-dione (150 mg, 0.173 mmol), 2,5-bis(trimethyl-stannyl)thiophene (70.7 mg, 0.173 mmol), tris(*o*-tolyl)phosphine (P(*o*-tolyl)$_3$) (10 mg) and tris(dibenzylidene acetone)dipalladium(0) ($Pd_2(dba)_3$) (6 mg) in anhydrous toluene (4 mL) were charged in a microwave reactor vial. After the reaction mixture was heated at 140 °C for 12 h, the mixture was poured into methanol (200 mL) and the precipitate was collected in a Soxhlet thimble filter. The precipitate was then extracted with methanol, acetone, hexane and chloroform. The chloroform solution was concentrated before it was precipitated in methanol. The precipitate was filtered over PTFE filter and dried overnight in 87% yield. PISe was synthesized by the same procedure as the method for synthesis of PIT except use of 2,5-bis(trimethyl-stannyl)selenophene instead of thiophene analogue. PITe was synthesized by reacting isoindigo and 2,5-bis(trimethyl-stannyl)tellurophene in the presence of tetrakis(triphenylphosphine)-palladium(0) ($Pd(PPh_3)_4$). The yields of PISe and PITe were 79% and 85%, respectively.

Characterization

The chemical structures of monomers were identified by ^1H NMR (Avance DPX-300) and ^{13}C NMR (Avance DPX-500). Mass analysis was performed on a mass analyzer (JMS-600W, JEOL). Molecular weight and its distribution were measured by gel permeation chromatography (GPC) (Waters) equipped with a Waters 2414 refractive index detector using $CHCl_3$ as an eluent, where the columns were calibrated against standard polystyrene samples. The optical absorption spectra were obtained by an UV–Visible spectrophotometer (Lambda 25, Perkin Elmer). Cyclic voltammetry experiments were carried out in an electrolyte solution of 0.1 M tetrabutylammonium hexafluorophosphate (Bu_4NPF_6) in acetonitrile. A three-electrode setup was used with platinum wires as both working and counter electrode. Ag/Ag^+ was used as the reference electrode calibrated with ferrocene/ferrocenyl couple (Fc/Fc^+). The HOMO energy levels was calculated from the onset point using the equation of $E_{HOMO} = -(4.8 + E_{ox})$. X-ray diffraction (XRD) patterns were obtained from an X-ray diffractometer (New D8 Advance, Bruker) using Cu-Kα radiation (λ= 1.5418 Å) at a scan rate of 2° min^{-1}. Thin film morphology was characterized by transmission electron microscopy (TEM) (JEOL, JEM1010) operating at 80 kV of acceleration voltage.

Device fabrication and Characterization

Photovoltaic devices were fabricated with a layered structure of ITO/ poly(3,4-ethylene dioxythiophene):poly(styrene sulfonate) (PEDOT:PSS)/polymer:$PC_{61}BM$/Ca/Al configuration. The ITO coated glass substrate was cleaned by stepwise sonication in acetone and isopropanol for 15 min each. After complete drying, the ITO coated glass substrate was treated with UV–ozone for 15 min. PEDOT:PSS was spin-coated onto the ITO with 40 nm in thickness, and the substrate was annealed at 150 °C for 10 min in a N_2-filled glove box. After a mixture of polymer and $PC_{61}BM$ was dissolved in anhydrous *o*-dichlorobenzene (*o*-DCB) under stirring at 70 °C for 4 h, the solution was spin-coated on the top of the PEDOT:PSS layer. Ca (20 nm in thickness) was thermally evaporated under vacuum (<10^{-6} Torr) on the top of the active layer before Al (100 nm) was thermally deposited on the Ca layer. The active area of cell was 4 mm^2. The photovoltaic performance was measured under nitrogen atmosphere inside the glove box. The current density–voltage (*J*–*V*) curve of the device was obtained on a computer-controlled Keithley 4200 source measurement unit under AM 1.5G (100 mW cm^{-2}) simulated by an Oriel solar simulator (Oriel 91160A). The light intensity was calibrated using a NREL-certified photodiode prior to each measurement. The EQE was measured using Polaronix K3100 IPCE measurement system (McScience). The light intensity at each wavelength was calibrated with a standard single-crystal Si cell. Bottom-gate/top-contact field-effect transistor (FET) was fabricated using heavily doped Si wafer as the bottom gate electrode and 250 nm of SiO_2 layer as the gate dielectric. The substrate was cleaned in piranha solution (H_2SO_4:H_2O_2 = 1:1) and then acetone for 20 min and dried in oven 120 °C for 1 h. The wafer was treated with UV–ozone for 20 min, and then the wafer was immersed in 0.1 mM octadecyltrichlorosilane (OTS) solution in anhydrous toluene. The polymer film was deposited on the OTS treated substrate by spin-coating the polymer solution (5 mg mL^{-1}) in $CHCl_3$, followed by thermal annealing at 150 °C under nitrogen atmosphere. After deposition of polymer thin film, the gold top contact with 40 nm in thickness was thermally evaporated in vacuum through a shadow mask. OFETs were characterized under nitrogen atmosphere using Keithley 4200 and MST5000A.

Table 1 Optical and electrochemical properties of polymers.

Polymer	M_n (kDa)	PDI	λ_{onset} (nm)		E_g^{opt} (eV)	HOMO (eV)	LUMO (eV)
			Solution	Film			
PIT	86	1.55	755	765	1.62	–5.61	–3.70
PISe	108	1.51	780	785	1.58	–5.66	–3.68
PITe	47	1.60	800	810	1.53	–5.69	–3.74

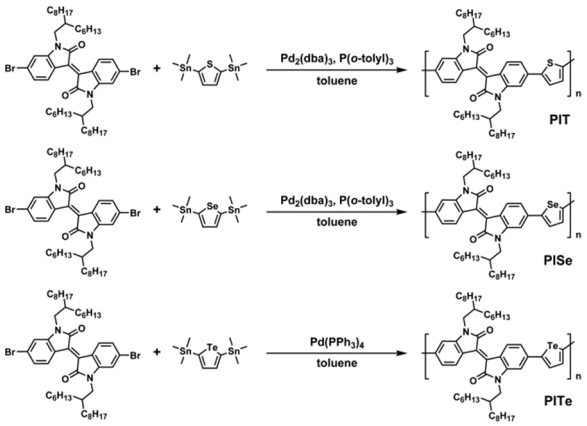

Scheme 1 Chemical structures and synthetic routes of PIT, PISe and PITe.

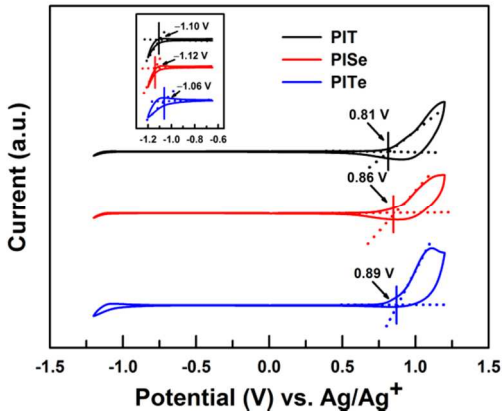

Fig. 2 Cyclic voltammograms of polymers films on platinum electrode.

RESULTS AND DISCUSSION

Synthesis and Charaterization

PIT and PISe were synthesized via the Stille coupling polycondensation catalyzed by $Pd_2(dba)_3$, while $Pd(PPh_3)_4$ was used as a catalyst to synthesize PITe (Scheme 1). All polymers are soluble in common organic solvents such as chloroform, tetrahydrofuran and chlorobenzene due to long and branched side chain on isoindigo unit. The number-average molecular weights (M_n) of PIT, PISe and PITe were 86, 108, and 47 kDa with polydispersity indexes (PDI) of 1.55, 1.51, and 1.60, respectively, as determined using GPC.

Optical and Electrochemical Properties

When the UV–Visible spectra of three polymers in solution are compared, as shown in Fig. 1a, it reveals that the absorption maximum (λ_{max}) and the absorption onset (λ_{onset}) of the three polymers are in the order of PITe, PISe and PIT, indicating that the bathochromic shift of PITe is the most prominent. The absorption spectra of the three polymers in solid state are red-shifted as compared to those in solution, as shown in Fig. 1b, while the λ_{max} and λ_{onset} of the three polymers in solid state shows the same order as in solution, indicating that the substitution of sulfur in thiophene with selenium and tellurium is an effective method to extend the absorption range to longer wavelength. Furthermore, the molar extinction coefficient of PISe (~64,000 $M^{-1}cm^{-1}$) is larger than that of PIT (~53,200 $M^{-1}cm^{-1}$), when the coefficient was calculated from the molarity of monomer units. When the HOMO energy levels of polymers were measured using cyclic voltammetry, as shown in Fig. 2, the HOMO energy levels of PIT, PISe and PITe were –5.61, –5.66 and –5.69 eV, respectively. These deep HOMO energy levels of polymers are expected to afford high open circuit voltage (V_{OC}) of PSCs.

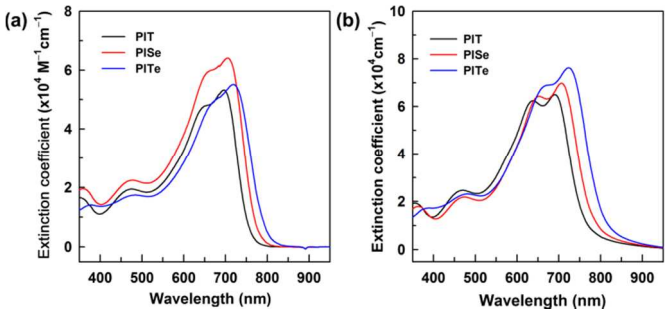

Fig. 1 UV–Vis absorption spectra of polymers (a) in $CHCl_3$ solution and (b) in film.

Photovoltaic Properties

The effect of chalcogen atom substitution on the photovoltaic properties was investigated by measuring and comparing the photovoltaic properties of the three polymers. The *J*–*V* curves of three devices are shown in Fig. 3a, and their photovoltaic parameters are summarized in Table 2. When the solar cell performances of three polymers are compared, the device fabricated from PISe exhibits the highest PCE value of 5.72% with a V_{OC} of 0.95 V, a J_{SC} of 10.21 mA cm^{-2} and a FF of 59% while the device from PITe shows the lowest PCE of 1.16%, although all devices fabricated from three polymers show nearly the same V_{OC} (0.91–0.95 V). The highest PCE of PISe

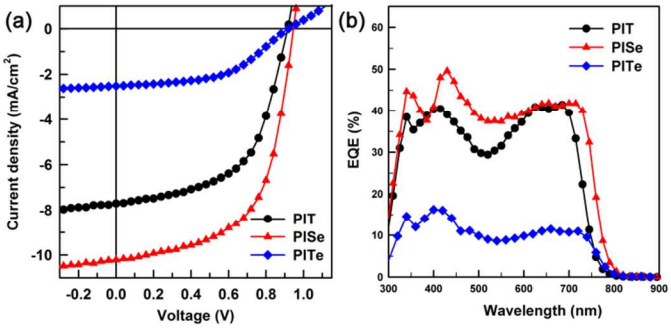

Fig. 3 (a) *J*–*V* curves under an AM 1.5G condition (100 mW cm^{-2}) and (b) EQE spectra of polymer solar cells.

Table 2 Photovoltaic properties of PIT, PISe and PITe blended with $PC_{61}BM$.

Polymer	Blend ratio[a]	V_{OC} (V)	J_{SC} (mA cm^{-2})	FF (%)	PCE[b] (%)
PIT	1:1	0.91	7.71	57	3.98 (3.94)
PISe	1:1	0.95	10.21	59	5.72 (5.69)
PITe	1:4	0.92	2.51	50	1.16 (1.07)

[a] Polymer:$PC_{61}BM$ blend ratios; [b] The PCE in parentheses are the average PCE from 4 devices.

arises mainly from the highest J_{SC}, which is attributed to effective photon absorption and high external quantum efficiency (EQE), as shown in Fig. 1a and 3b. However, comparison of the absorption spectra (Fig. 1a) with the external quantum efficiency spectra (Fig. 3b) reveals that the PITe-based device exhibits a low EQE although PITe has the lowest band-gap and thus is expected to absorb more photons at longer wavelengths than others. It should be mentioned here that higher PCE of PISe does not arise mainly from its higher molecular weight, because the PCE of PISe does not significantly depend upon the molecular weight when the molecular weight exceeds 40 kDa (see Figure S5 and Table S1 in Electronic Supplementary Information).

Crystallinity of Polymers and OFET Properties

To investigate the reason for lower J_{SC} than expected for PITe, we measured the crystallinity and charge transport properties of the polymers by X-ray diffraction (XRD) and FET method. The XRD spectra (Fig. 4) of three polymers reveal that PIT and PISe show a weak diffraction peak of (100) while PITe exhibits a strong diffraction peak of (100) along with discernible (200) and (300) peaks, indicating that PITe has the highest crystallinity. In other words, the degree of crystallinity is in the order of PITe, PISe and PIT. When the FET mobilities of three polymers were measured with the bottom-gate and top-contact configuration (Fig. 5), the FET hole mobilities of PIT, PISe and PITe were 0.003, 0.016 and 0.072 cm^2 V^{-1} s^{-1}, respectively, indicating that the hole mobility is closely related to the crystallinity. It has also been reported that tellurophene-containing conjugated polymer has higher FET hole mobility than its thiophene analogue.[46] Therefore, it is concluded that the low J_{SC} of PITe is not related to the crystallinity and the hole mobility of polymer, because PITe has higher hole mobility

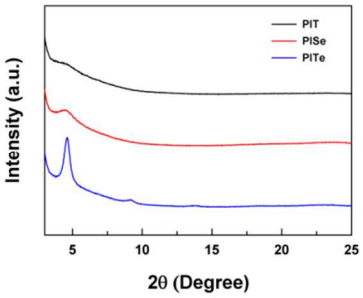

Fig. 4 X-ray diffraction patterns of the polymers in solid films.

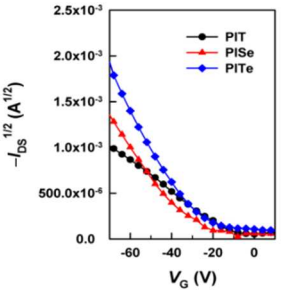

Fig. 5 Transfer curves of field-effect transistors fabricated from PIT, PISe and PITe.

than PIT and PISe, but exhibits the lowest J_{SC}. Hence, another factor must be considered for low J_{SC} of PITe.

Thin Film Morphology

Another important factor to control J_{SC} is the morphology of active layer in PSC device. When the TEM images of the three active layers are compared, as shown in Fig. 6, it reveals that the image of PISe:$PC_{61}BM$ blend exhibits finer domains while the image of PITe:$PC_{61}BM$ blend shows larger and coarse phase separation, which may negatively contribute to J_{SC}, impeding effective charge carrier transport. The inferior morphology of PITe:$PC_{61}BM$ film might result from excessive aggregation of PITe due to strong Te···Te intermolecular interactions[27] and/or poor miscibility between PITe and $PC_{61}BM$.[50] It should be noted here that all the devices were optimized by varying the blend ratio of polymer to $PC_{61}BM$ and adding a small amount of 1,8-diiodooctane (DIO). Therefore, it is concluded that the highest J_{SC} of PISe arises mainly from effective photon absorption at long wavelength region and effective charge transport due to fibrillar morphology with finer

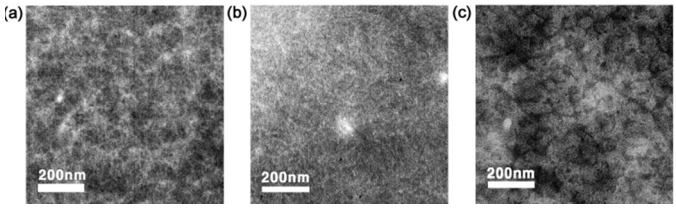

Fig. 6 TEM images of blend films of (a) PIT:$PC_{61}BM$ (1:1, w/w), (b) PISe:$PC_{61}BM$ (1:1, w/w) and (c) PITe:$PC_{61}BM$ (1:4, w/w) fabricated from *o*-DCB in the presence of 2.5 vol% of DIO.

domains whereas the lowest J_{SC} of PITe-based solar cell is mainly attributed to the coarse morphology with large phase separation.

Conclusions

In this study, a series of low band-gap conjugated copolymers composed of isoindigo and aromatic heterocyclic compounds with different chalcogen atoms were synthesized to investigate the effect of different chalcogen atom on their photovoltaic performances. As the thiophene unit in isoindigo-based conjugated polymer was substituted by selenophene and tellurophene, the band-gap and HOMO energy level of the conjugated copolymer becomes lower and deeper, respectively, and the crystallinity of the polymer is increased. The solar cell device based on PISe exhibits the highest PCE of 5.72% with a high V_{OC} of 0.95 V due to deep HOMO level and the highest J_{SC} of 10.21 mA cm^{-2} due to effective absorption of long wavelength region and formation of fibrillar morphology with finer domains, whereas the PITe-based PSC shows the lowest PCE of 1.16% with the lowest J_{SC} of 2.51 mA cm^{-2} due to coarse morphology with large phase separation, although the PITe thin film exhibits the highest FET hole mobility of 0.072 $cm^2 V^{-1} s^{-1}$ due to the highest crystallinity.

Acknowledgements

The authors thank the Ministry of Education, Science and Technology, Korea for financial support through the Global Research Laboratory (GRL) program.

Notes and references

Department of Materials Science and Engineering, Seoul National University, 1 Gwanak-ro, Gwanak-gu, Seoul 151-744, Korea. E-mail: whjpoly@snu.ac.kr

1 S. R. Forrest, *Nature*, 2004, **428**, 911–918.
2 F. C. Krebs, *Sol. Energy Mater. Sol. Cells*, 2009, **93**, 394–412.
3 Z. Fan, H. Razavi, J. Do, A. Moriwaki, O. Ergen, Y.-L. Chueh, P. W. Leu, J. C. Ho, T. Takahashi, L. A. Reichertz, S. Neale, K. Yu, M. Wu, J. W. Ager and A. Javey, *Nat. Mater.*, 2009, **8**, 648–653.
4 N. S. Lewis, *Science*, 2007, **315**, 798–801.
5 J. W. Jung and W. H. Jo, *Adv. Funct. Mater.*, 2010, **20**, 2355–2363.
6 M. Kaltenbrunner, M. S. White, E. D. Głowacki, T. Sekitani, T. Someya, N. S. Sariciftci and S. Bauer, *Nat. Commun.*, 2012, **3**, 770–776.
7 J. W. Jung, F. Liu, T. P. Russell and W. H. Jo, *Energy Environ. Sci.*, 2012, **5**, 6857–6861.
8 K.-H. Ong, S.-L. Lim, H.-S. Tan, H.-K. Wong, J. Li, Z. Ma, L. C. H. Moh, S.-H. Lim, J. C. de Mello and Z.-K. Chen, *Adv. Mater.*, 2011, **23**, 1409–1413.
9 Y. Li, *Acc. Chem. Res.*, 2012, **45**, 723–733.
10 P.-L. T. Boudreault, A. Najari and M. Leclerc, *Chem. Mater.*, 2011, **23**, 456–469.
11 H. Zhou, L. Yang, and W. You, *Macromolecules*, 2012, **45**, 607–632.
12 Y. Li, P. Sonar, L. Murphy and W. Hong, *Energy Environ. Sci.*, 2013, **6**, 1684–1710.
13 J. Mei, K. R. Graham, R. Stalder and J. R. Reynolds, *Org. Lett.*, 2010, **12**, 660–663.
14 E. H. Jung and W. H. Jo, *Energy Environ. Sci.*, 2014, **7**, 650–654.
15 Y. Deng, J. Liu, J. Wang, L. Liu, W. Li, H. Tian, X. Zhang, Z. Xie, Y. Geng and F. Wang, *Adv. Mater.*, 2014, **26**, 471–476.
16 Z. Ma, D. Dang, Z. Tang, D. Gedefaw, J. Bergqvist, W. Zhu, W. Mammo, M. R. Andersson, O. Inganäs, F. Zhang and E. Wang, *Adv. Energy Mater.*, 2014, DOI: 10.1002/aenm.201301455.
17 E. Wang, Z. Ma, Z. Zhang, K. Vandewal, P. Henriksson, O. Inganäs, F. Zhang and M. R. Andersson, *J. Am. Chem. Soc.*, 2011, **133**, 14244–14247.
18 L. Fang, Y. Zhou, Y.-X. Yao, Y. Diao, W.-Y. Lee, A. L. Appleton, R. Allen, J. Reinspach, S. C. B. Mannsfeld and Z. Bao, *Chem. Mater.*, 2013, **25**, 4874–4880.
19 C.-C. Ho, C.-A. Chen, C.-Y. Chang, S. B. Darling and W.-F. Su, *J. Mater. Chem. A*, 2014, **2**, 8026–8032.
20 Z. Ma, W. Sun, S. Himmelberger, K. Vandewal, Z. Tang, J. Bergqvist, A. Salleo, J. W. Andreasen, O. Inganäs, M. R. Andersson, C. Müller, F. Zhang and E. Wang, *Energy Environ. Sci.*, 2014, **7**, 361–369.
21 E. Wang, Z. Ma, Z. Zhang, P. Henriksson, O. Inganäs, F. Zhang and M. R. Andersson, *Chem. Commun.*, 2011, **47**, 4908–4910.
22 J. W. Jung, F. Liu, T. P. Russell and W. H. Jo, *Energy Environ. Sci.* 2013, **6**, 3301–3307.
23 Y. Yang, R. Wu, X. Wang, X. Xu, Z. Li, K. Li and Q. Peng, *Chem. Commun.*, 2014, **50**, 439–441.
24 R. Stalder, J. Mei, K. R. Graham, L. A. Estrada and J. R. Reynolds, *Chem. Mater.*, 2014, **26**, 664–678.
25 E. Wang, W. Mammo and M. R. Andersson, *Adv. Mater.*, 2014, **26**, 1801–1826.
26 P. Deng and Q. Zhang, *Polym. Chem.*, 2014, **5**, 3298–3305.
27 A. Patra and M. Bendikov, *J. Mater. Chem.*, 2010, **20**, 422–433.
28 H. A. Saadeh, L. Lu, F. He, J. E. Bullock, W. Wang, B. Carsten and L. Yu, *ACS Macro Lett.*, 2012, **1**, 361–365.
29 M. Shahid, R. S. Ashraf, Z. Huang, A. J. Kronemeijer, T. McCarthy-Ward, I. McCulloch, J. R. Durrant, H. Sirringhaus and M. Heeney, *J. Mater. Chem.*, 2012, **22**, 12817–12823.
30 B. Kim, H. R. Yeom, M. H. Yun, J. Y. Kim and C. Yang, *Macromolecules*, 2012, **45**, 8658–8664.
31 L. Dou, W.-H. Chang, J. Gao, C.-C. Chen, J. You and Y. Yang, *Adv. Mater.*, 2013, **25**, 825–831.
32 T. Earmme, Y.-J. Hang, N. M. Murari, S. Subramaniyan and S. A. Jenekhe, *J. Am. Chem. Soc.*, 2013, **135**, 14960–14963.
33 D. H. Wang, A. Pron, M. Leclerc and A. J. Heeger, *Adv. Funct. Mater.*, 2013, **23**, 1297–1304.
34 S. S. Zade, N. Zamoshchik and M. Bendikov, *Chem. Eur. J.*, 2009, **15**, 8613–8624.
35 J. Casado, M. M. Oliva, M. C. R. Delgado, R. P. Ortiz, J. J. Quirante, J. T. L. Navarrete, K. Takimiya and T. Otsubo, *J. Phys. Chem. A*, 2006, **110**, 7422–7430.
36 U. Salzner, J. B. Lagowski, P. G. Pickup and R. A. Poirier, *Synth. Met.*, 1998, **96**, 177–189.
37 S. Glenis, D. S. Ginley and A. J. Frank, *J. Appl. Phys.*, 1987, **62**, 190–194.
38 Y. Wang, S. R. Parkin and M. D. Watson, *Org. Lett.*, 2008, **10**, 4421–4424.

39 E. I. Carrera, T. M. McCormick, M. J. Kapp, A. J. Lough and D. S. Seferos, *Inorg. Chem.*, 2013, **52**, 13779–13790.
40 G. He, L. Kang, W. T. Delgado, O. Shynkaruk, M. J. Ferguson, R. McDonald and E. Rivard, *J. Am. Chem. Soc.*, 2013, **135**, 5360–5363.
41 M. Lapkowski, R. Motyka, J. Suwiński and P. Data, *Macromol. Chem. Phys.*, 2012, **213**, 29-35.
42 T. Otsubo, S. Inoue, H. Nozoe, T. Jigami and F. Ogura, *Synth. Met.*, **69**, 537-538.
43 A. A. Jahnke, B. Djukic, T. M. McCormick, E. B. Domingo, C. Hellmann, Y. Lee and D. S. Seferos, *J. Am. Chem. Soc.*, 2013, **135**, 951–954.
44 X. Guo, R. P. Ortiz, Y. Zheng, M.-G. Kim, S. Zhang, Y. Hu, G. Lu, A. Facchetti and T. J. Marks, *J. Am. Chem. Soc.*, 2011, **133**, 13685–13697.
45 A. A. Jahnke, G. W. Howe and D. S. Seferos, *Angew. Chem. Int. Ed.*, 2010, **49**, 10140–10144.
46 M. Kaur, D. S. Yang, J. Shin, T. W. Lee, K. Choi, M. J. Cho and D. H. Choi, *Chem. Commun.*, 2013, **49**, 5495–5497.
47 D. P. Sweat and C. E. Stephens, *J. Organomet. Chem.*, 2008, **693**, 2463–2464.
48 D. E. Seitz, S. H. Lee, R. N. Hanson and J. C. Bottaro, *Synth. Commun*., 1983, **13**, 121–128.
49 D. P. Sweat and C. E. Stephens, *Synthesis* 2009, **19**, 3214–3218.
50 Z. Ma, E. Wang, K. Vandewal, M. R. Andersson and F. Zhang, *Appl. Phys. Lett.*, 2011, **99**, 143302–143304.

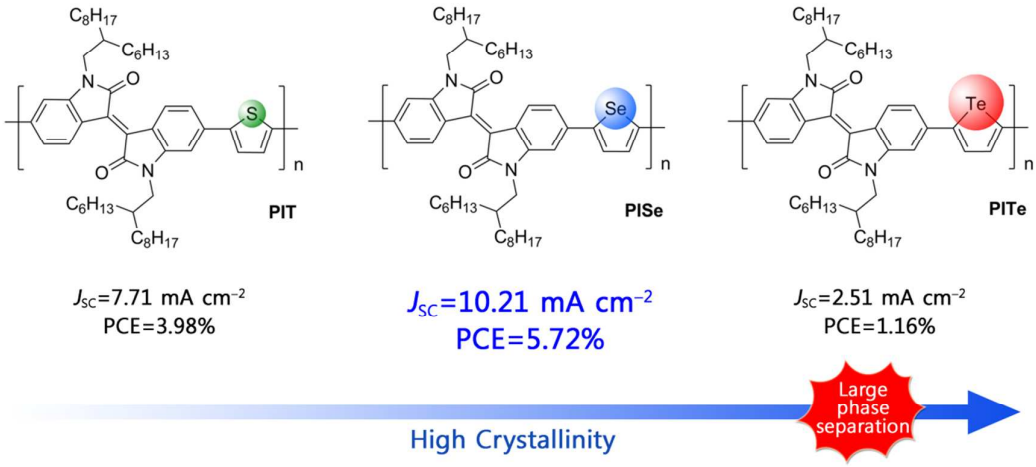

Three low bandgap conjugated copolymers based on isoindigo and three different chalcogenophenes (thiophene, selenophene and tellurophene) were synthesized to investigate the effect of different chalcogenophene on their photovoltaic properties.